Journal of Engineering Science and Technology
Vol. 4, No. 1 (2009) 111 - 121

STUDY OF DEFECT ADMISSIBILITY IN GAS PIPELINES BASED ON FRACTURE MECHANICS

N. ABDELBAKI, E. BOUALI, M. GACEB, M. BETTAYEB*

Laboratoire Fiabilité des Equipements Pétroliers & Matériaux
Faculté des Hydrocarbures et de la Chimie, Université M'Hamed Bougara de Boumerdès,
Avenue de l'indépendance, Boumerdès -35000, Algerie
*Corresponding Author: lfep@umbb.dz

Abstract

Bearing in mind the considerable distances between natural gas fields and consumers' appliances, transport by gas pipelines remains the most competitive means. These gas pipelines which are generally made of steel pipes may contain however several types of defects of various origins and which are susceptible to initiate cracks which may grow under some circumstances to such extent as to lead to fracture. Failures of gas pipelines may have serious consequences and may lead to catastrophes from ecological and financial viewpoints. It is therefore interesting to study the defect admissibility so as to maximize safety and minimize exploitation costs through a simplified method based on the Failure Assessment Diagram (FAD). The latter is used in conjunction with Finite Element Analysis (FEM) applied to fracture mechanics to help decision making as to whether a given defect present in a pipe is acceptable or not.

Keywords: Cracks, Finite elements, Gas pipelines, FAD.

1. Introduction

Increase in gas pipelines' capacities has brought to the forefront, questions related to reliability and ecological safety. In the working of gas pipelines, as short as they may be, stoppages and furthermore failures, lead to important economical and ecological losses.

The reliability of linear sections of gas pipelines represent the prerequisite condition for their economicity, given that it depends on consumers' safe and continuous supply in natural gas. On another hand, their safety and particularly

Nomenclatures

a_c	Critical length of crack, m
D	Pipe's diameter, m
E	Young's elastic modulus, MPa
J^o	Rice's J integral
K_I	Stress intensity factor, MPa $\sqrt{m}$
K_{IC}	Material toughness, MPa $\sqrt{m}$
P	Service pressure, Pa
R_{in}	Internal radius of pipe, m
t	Pipe wall thickness, m

Greek Symbols

μ	Shear modulus, GPa
ν	Poisson's ratio
σ_f	Average flow stress, MPa
σ_n	Stress in the ligament ahead of the defect, MPa
σ_u	Ultimate tensile strength, MPa
σ_y	Yield strength, MPa

the protection of environment from potential danger, caused by explosions or fire is an obligatory condition. In this context, questions of detection, elimination of gas pipeline ruptures causes, and research activities related to this field have a great practical importance. The presence of cracks in gas pipeline pipes is related to several causes such as inclusions, micro-voids, manufacturing defects, overloads amongst others. It becomes necessary therefore, to provide answers to preoccupations about crack harm. Within this context, we have associated, in this paper, fracture mechanics with SAMCEF program in order to differentiate between harmful cracks and those which may subsist in pipes. The case of 42" (1066.8 mm)-diameter X52 steel gas pipeline is considered.

2. Ruptures in Pipes

Sources of failures in gas pipelines are of various natures. They may appear as total ruptures or just as leaks. Most of these failures are caused by corrosion bites or by stress corrosion cracking. There exist however, problems attached to weld defects. Soil movements (ground slips, earthquakes…) may also be sources of damage to underground gas pipelines. Gas pipelines users have been studying these problems for a long time and have a good knowledge about methods to manage the problems. But external aggressions should really not be neglected. In effect, it may happen that gas pipelines are damaged or even perforated accidentally during excavation works by heavy field engines for example.

Fatigue crack initiation problems and ruptures initiated from stress concentration sites account for more than 90% of service failures. The presence of geometrical discontinuity such as a notch will lead to the weakening of gas pipelines fracture strength. This may be explained by the resulting reduction in

section of the pipe making it more sensitive to service pressures and to efforts caused by soil movements, followed by an exponential extension of the defect by local stress amplification effect [1].

The presence of defects is generally detected by non destructive testing of the finished structure. The industrial problem is to control rupture risks due to the presence of defects in structures. Wherever a defect is detected in structures three attitudes may be considered:

- Conserving the defect as it is while continuing to use the equipment.
- Repairing bearing in mind, however that this may lead to other defects which may be more severe.
- Replacing the defected part or section

In order to make a right decision, there exist various methods of assessment of defect nocivity. Amongst these we can cite [2]:

- The two criteria or modified R6 method.
- The PD6493 (1991) recommendation or its recent version BS 7910(1999).

According to these two methods, the treatments of defect acceptability, in terms of rupture risks, is based on the failure assessment diagram.

3. Failure Assessment Diagram

This diagram needs the calculation of two parameters corresponding respectively to brittle fracture risk K_r (y-axis) and plastic ruin S_r (x-axis) for each defect. These parameters are calculated by the following expressions [3]

Brittle fracture: $$K_r = \frac{K_I}{K_{IC}} \quad (1)$$

Plastic ruin: $$S_r = \frac{\sigma_n}{\sigma_f} \quad (2)$$

where, σ_f is equal to $\frac{\sigma_y + \sigma_u}{2}$ for $\sigma_f < 1.2\ \sigma_y$ and equal to $1.2\ \sigma_y$ otherwise.

A boundary envelope is then defined by a relation of the form $K_r = f(S_r)$. The graphical representation of the relation in the referential (K_r, S_r) constitutes the failure assessment diagram (FAD). A defect therefore is acceptable if the calculated pair (K_r, S_r) is located under the curve $K_r = f(S_r)$ in the FAD. According to British Standards, PD6493 recommendation applies to:

- welded martensitic and austenitic aluminium alloy structures,
- volume defects,
- different failure modes.

Different levels of investigation are proposed [4, 5]. Figure 1 presents three levels (1, 2 and 3).

Level 1: The most basic, is applicable in the case of brittle fracture (Linear Elastic Fracture Mechanics). Required necessary data on materials are limited and the investigation is rapid.

Level 2: Does not require taking into account the safety factor which is accounted for by the maximizing of the stresses and defect dimensions and by the minimizing of mechanical properties.
Level 3: Can be used when the failure is preceded by strong plastic deformation.

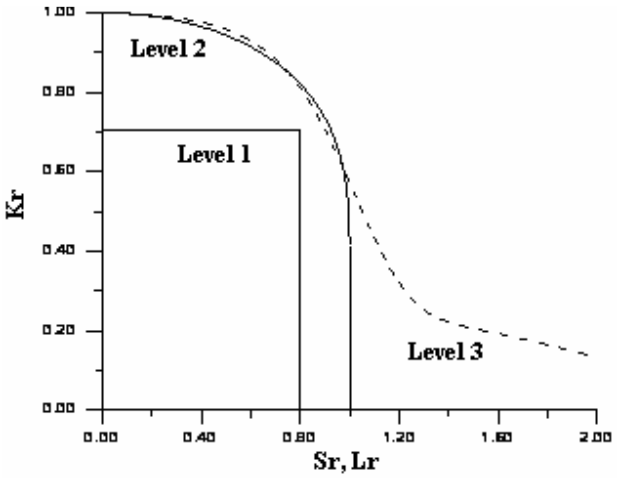

Fig. 1. FAD for Three Possible Investigation Levels (PD6493).

The equations defining the acceptability envelope for each level are given by the following expressions:
Level 1 $K_r < 0.707$ for $S_r < 0.8$ and $K_r = 0$ for $S_r > 0.8$

$$\left.\begin{aligned} \text{Level 2} \quad & K_r = S_r \left[\frac{8}{\pi^2} \ln\left(\frac{1}{\cos\left(\frac{\pi}{2} S_r \right)} \right) \right]^{-0.5} \\ \text{Level 3} \quad & K_r = \left[\frac{E \ln(1+\varepsilon)}{\sigma(1+\varepsilon)} + \frac{\sigma^3 (1+\varepsilon)^3}{2\sigma_y^2 E \ln(1+\varepsilon)} \right]^{-0.5} \end{aligned}\right\} \tag{3}$$

It should be noted that a rational tensile curve of the material in which the defect exists is necessary. This curve allows to establish a relationship $\sigma = f(\varepsilon)$ used in Eqs. (3). In the case of investigation levels 1 and 2 only data such as σ_y and σ_u are necessary. The S_r parameter is replaced by $L_r = \dfrac{\sigma(1+\varepsilon)}{\sigma_y}$ to characterize rupture by generalized plasticity.

We also give K_r, for level 3 by the relationship:

$$K_r = \left(1 - 0.14 L_r^2\right)\left[0.3 + 0.7 * \exp\left(-0.65 L_r^6\right)\right] \tag{4}$$

4. Finite Element Method Calculation [6,7]

The calculation of parameter K_r is based on calculation of the stress intensity factor *K* at the crack tip. It constitutes one of the most important parts of fracture mechanics. For cracks of usual geometry where the analytical or approximate solution is known, curves or abacuses necessary for calculation can be proposed to designers of formulas lists. For cracks of more complex geometry, we have to use numerical methods of calculation such as the finite element method which is a standard method for numerical analysis of fracture mechanics problems.

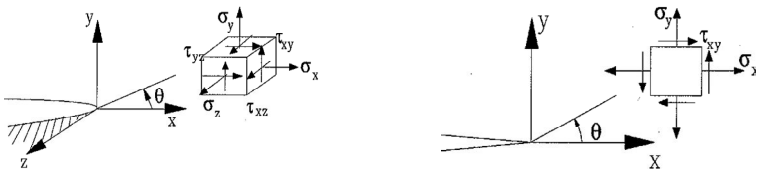

a- In 3D b- In 2D

Fig. 2. Stress Fields ahead of Crack Tips.

According to Irwin stress and displacement fields at the crack tip vicinity at a point (r, θ) (Fig. 2) are given by expressions (5) and (6) bellow:

$$\left.\begin{aligned}
\sigma_x &= \frac{1}{\sqrt{2\pi r}}\left[K_I\cos\frac{\theta}{2}\left(1-\sin\frac{\theta}{2}\sin\frac{3\theta}{2}\right)-K_{II}\sin\frac{\theta}{2}\left(2+\cos\frac{\theta}{2}\cos\frac{3\theta}{2}\right)\right]\\
\sigma_y &= \frac{1}{\sqrt{2\pi r}}\left[K_I\cos\frac{\theta}{2}\left(1+\sin\frac{\theta}{2}\sin\frac{3\theta}{2}\right)+K_{II}\sin\frac{\theta}{2}\cos\frac{\theta}{2}\cos\frac{3\theta}{2}\right]\\
\sigma_z &= \frac{3-\nu-\kappa-\nu\kappa}{4\nu}\left(\sigma_x+\sigma_y\right)\\
\tau_{xy} &= \frac{1}{\sqrt{2\pi r}}\left[K_I\sin\frac{\theta}{2}\cos\frac{\theta}{2}\cos\frac{3\theta}{2}+K_{II}\cos\frac{3\theta}{2}\left(1-\sin\frac{\theta}{2}\sin\frac{3\theta}{2}\right)\right]\\
\tau_{yz} &= \frac{K_{III}}{\sqrt{2\pi r}}\cos\frac{\theta}{2}\\
\tau_{zx} &= -\frac{K_{III}}{\sqrt{2\pi r}}\sin\frac{\theta}{2}
\end{aligned}\right\} \quad (5)$$

$$\left.\begin{aligned}
u &= \frac{K_I}{4\mu}\sqrt{\frac{2r}{\pi}}\left[(\kappa-1)\cos\frac{\theta}{2}+\sin\theta\sin\frac{\theta}{2}\right]+\frac{K_{II}}{\mu}\sqrt{\frac{2r}{\pi}}\left[(\kappa+1)\sin\frac{\theta}{2}+\sin\theta\cos\frac{\theta}{2}\right]\\
v &= \frac{K_I}{4\mu}\sqrt{\frac{2r}{\pi}}\left[(\kappa+1)\sin\frac{\theta}{2}-\sin\theta\sin\frac{\theta}{2}\right]+\frac{K_{II}}{\mu}\sqrt{\frac{2r}{\pi}}\left[(-\kappa+1)\cos\frac{\theta}{2}+\sin\theta\sin\frac{\theta}{2}\right]\\
w &= \frac{K_{III}}{\mu}\sqrt{\frac{2r}{\pi}}\sin\frac{\theta}{2}
\end{aligned}\right\} \quad (6)$$

where $\mu = \dfrac{E}{2(1+\nu)}$ (7)

For plane strain $\kappa = 3-4\nu$ (8)

For plane stress $\kappa = \dfrac{3-\nu}{1+\nu}$ (9)

K_I, K_{II}, and K_{III} are stress intensity factors for three fracture modes I, II, and III.

Mechanical fields' singularities at the crack tip are always of the type $u \approx \sqrt{r}$ for displacements and $1/\sqrt{r}$ for stresses. The use of the finite elements method in the study of cracking takes two distinct considerations into account.

4.1. Modelling of the crack tip singularity

To represent singularities of the stress and displacements fields in a convenient manner, special crack elements are used for direct modelling of the singularities at the vicinity of the crack tip using degenerated isoparametric elements for the singular field (Fig. 3).

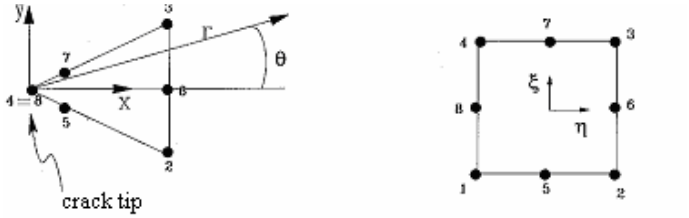

Fig. 3. Degenerated Quadrilateral Element.

4.2. Finite elements analysis results interpretation

Following finite element analysis, a means should be found for stress intensity factor evaluation from the stress and displacement fields' results. There exists a global approach which consists of calculating stress intensity factors starting from the value of an independent integral of integration contour such as Rice's J integral (Fig. 4).

Physically, it describes the rate of potential energy change corresponding to a small increase in crack length and is given in the form:

$$J = \int_{\Gamma} (U dy - t_i \frac{\partial u_i}{\partial x} ds) \quad (10)$$

where:

U	is the strain energy density
t_i	is the traction vector
u	is the displacement vector
ds	is an arc element along the integration contour Γ.

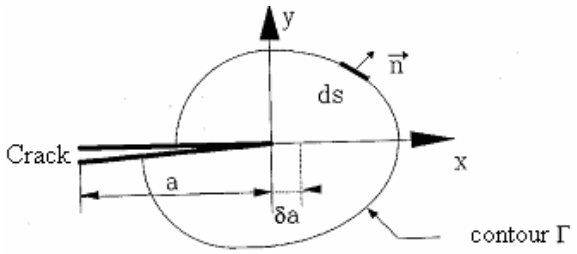

Fig. 4. Integration Contour.

In the following we will concern ourselves only with the first mode of fracture (opening mode *I*). The stress intensity factor K_I is given in terms of the J-integral by:

$$K_I = \sqrt{\frac{J * E}{1-\nu^2}} \tag{11}$$

5. Case study

We suppose the existence of an axial edge crack (defect) of length "a", in a pipe of diameter *D* subjected to an internal service pressure *P* as shown in Fig. 5.

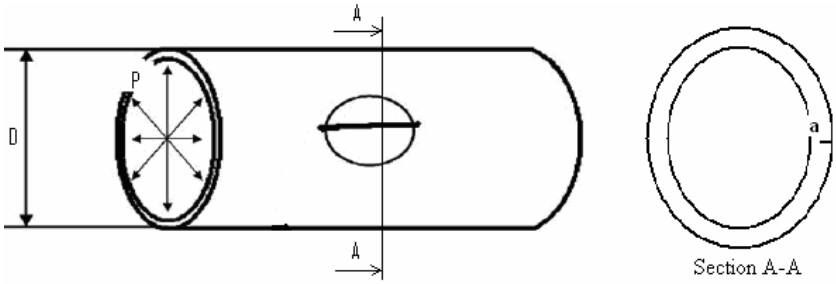

Fig. 5. Pipe with External Surface Crack.

5.1. Geometry and mechanical properties of the pipe under study

In our study we have considered an X52 steel gas pipeline pipe with diameter *D*=1066.8 mm (42'') and thickness *t*=16.16 mm with a Poisson's ratio of $\nu = 0.3$. The steel used for the pipe has the following mechanical properties (Table 1).

Table 1. Mechanical Characteristics of the Pipe Steel.

Young's Modulus, *E*	Yield Strength	Maximal Strength	Toughness
MPa	MPa	MPa	MPa $\sqrt{m}$
203000	410	528	120

5.2. Finite elements modelling

A computer program called SAMCEF [8] has been used for modelling and calculations. Idealization of the pipe has been made in such a way as to best represent the details of its construction, from the geometry as well as the mechanical points of view. We have identified a problem for study such as that of plane strain state. And as the problem is symmetrical, the meshing has been done only on half of the pipe using pre-processor called BACON. We used some finite elements included in the library of SAMCEF code such as isoparametric finite elements of type 15 (8 node quadrilateral elements) for the regular field away from the crack and degenerated finite elements for singular field at the crack tip while refining the meshing near the crack tip which represents the critical zone of the pipe (Fig. 6).

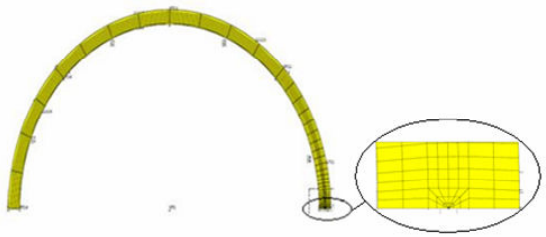

Fig. 6. Pipe Meshing and Mesh Refinement around the Crack.

6. Results and Discussion

6.1. Calculation of factor K_I

Computation has been carried out for different *a*/*t* ratios (0.2, 0.3, 0.4, 0.5, 0.6 and 0.7). Results for K_I (MPa $\sqrt{m}$) are given for a service pressure P = 60 bar and for two different pipe wall thicknesses (Fig. 7) and for a thickness of t =16.16 mm, the calculation is done for P = 60 bar and P = 70 bar (Fig. 8).

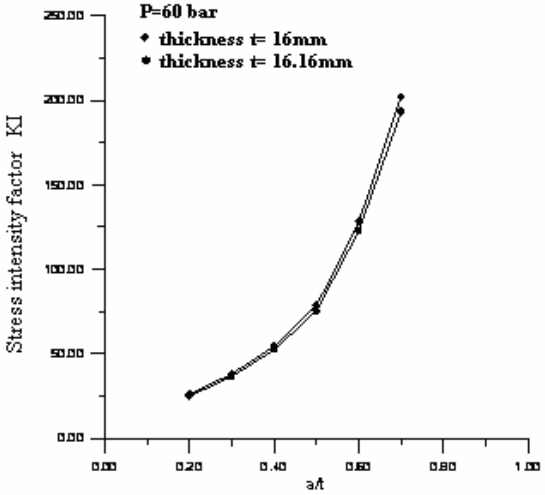

Fig. 7. Variation of Stress Intensity Factor with *a/t* Ratio for Two Different Pipe Wall Thicknesses.

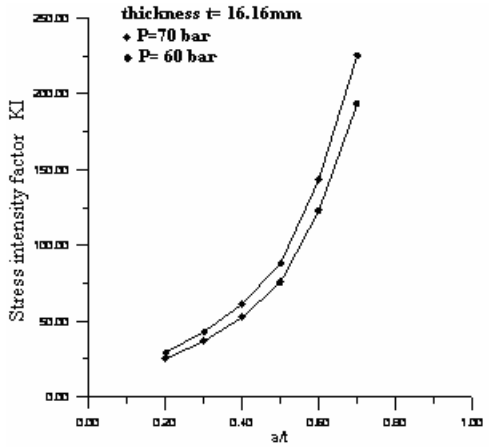

Fig. 8.Variation of Stress Intensity Factor with *a/t* Ratio for Different Pressures.

According to Figs. 7 and 8, we note that the stress intensity factor increases with increase in service pressure. This increase is even more significant for larger defect sizes (i.e. higher *a*/*t* ratios). This is of course logical since the more the pipe wall section is reduced by the crack, the more sensitive to service pressure it becomes which leads to a stress amplification effect which increases the stress intensity factor up to a critical value $K_I = K_{IC}$ (risk of brittle fracture).

With K_{IC} = 120 MPa$\sqrt{m}$ for P = 60 bar, a_C = 9.534 mm and a/t = 0.59 and for P = 70 bar, a_C = 8.89 mm and a/t = 0.55. On the other hand for a small thickness reduction, the increase of stress intensity factor is less important especially for small crack sizes. To take the risk of brittle fracture into account, we should calculate factor S_r for plastic ruin. To do so, a FAD diagram is drawn, by calculating factor K_r, Eq. (1).

6.2. Calculation of factor S_r

Factor S_r is calculated by Eq. (2) up to a ratio a/t = 0.6. σ_f is equal to 469 MPa and σ_n is equal to the hoop stress in the pipe which is exerted on the axial crack through the wall thickness and is given by:

$$\sigma_n = \frac{PR_{in}}{(t-a)} \tag{12}$$

6.3 FAD diagram

From the calculus of the pair (K_r, S_r) for ratios a/t = (0.2, 0.3, 0.4, 0.5 and 0.6) the diagram is drawn in Fig. 9.

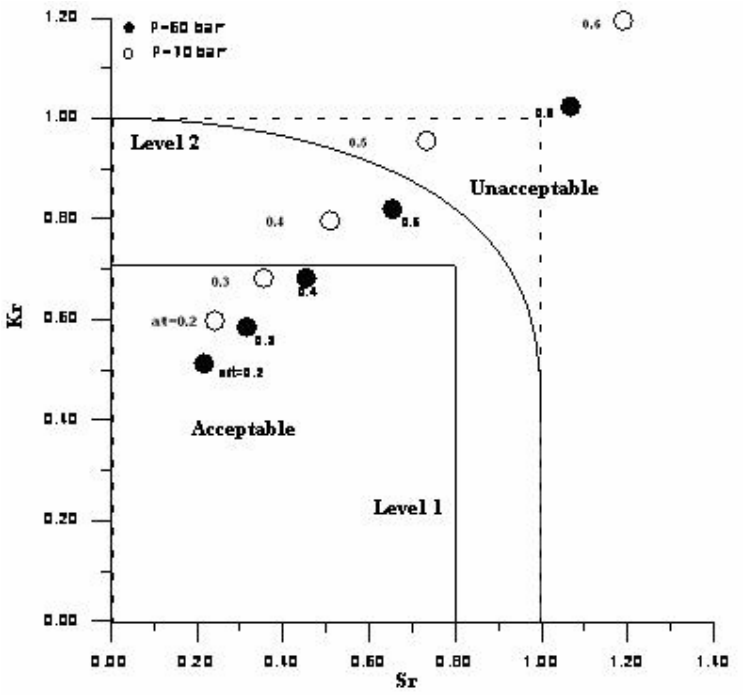

Fig. 9. FAD Diagram for Service Pressures of 60 bar and 70 bar.

The acceptable defect analysis has been achieved at level 1, since level 2 takes into consideration the possibility that fracture may not be totally brittle and that some ductile tearing may take place. We should therefore take into account small plastic deformations at crack tip in the calculation especially for stresses σ_n which increase above the yield strength.

According to this diagram, we notice a strong influence of crack length especially with increase in service pressure and the crack show very significant threat even more in the direction S_r. From this diagram we can select acceptable defects which should lie inside the admissible domain from those unacceptable ones. In this case study we can select those defects which are inside domain of level 2, because the yield strength has not been reached.

7. Conclusions

By establishing a diagram of defect admissibility (FAD), we have been able to decide rapidly, given a simple level of investigation, about acceptability of a type of defects in gas pipelines' pipes and thus seek maximum security. This diagram can be used as a tool for decision making about repairing or not of the damaged gas pipeline section. It makes it possible therefore to minimize gas pipeline exploitation costs. To be more precise in the decision, it is preferable to extend investigation to other types of defects which require analysis at level 3 according to recommendation (PD6493), or other recommendations.

References

1. Capelle, J. (2005). Caractérisation de la durée de vie des aciers à gazoducs par une approche déterministe. *Demi Journée Thématique sur la Sécurité et Transport de l'Hydrogène*. Forum ALPHEA sur l'Hydrogène. Metz, France, 17-28.
2. Blondeau, R.; and Lieurade, H.P. (2001). *Métallurgie et Mécanique du Soudage*. Paris: Ed Hermès.
3. Roche, R. (1995). Estimation pratique par la méthode des deux critères. *Journée d'Information sur l'Admissibilité des Défauts dans les Structures*, organisé par le CETIM. Senlis, France, 79-89.
4. Minerals Management Service. (2000). Appraisal and Development of Pipeline Defect, Assessment Methodologies. Final Report Phases I & II. Ascot, Berkshire: *MSL Engineering Limited*, 61-93.
5. Lee, J.S.; Ju, J.B.; Jang, J.I.; Kim, W.S; and Kwon, D. (2004). Weld crack assessments in API X65 pipeline, failure assessment diagrams with variations in representative mechanical properties. *Material Science and Engineering. A*, 373(1-2), 122-130.
6. Nguyen, D.H. (1998) Eléments de mécanique de la rupture. LTAS, Université de Liège. Personal communication.
7. Bettayeb, M. (2001). Etude de la fissuration du verre composite due à un impact à vitesse modérée. *Mémoire de D.E.S*, LTAS, Université de Liège.
8. SAMTECH. (2000) Manuel d'utilisation du code SAMCEF.